

Phonon Softening near structural transition in BaFe_2As_2 observed by inelastic x-ray scattering

Jennifer L. Niedziela,^{1,2,*} D. Parshall,^{1,†} K. A. Lokshin,³ A. S. Sefat,² A. Alatas,⁴ and T. Egami^{1,2,3}

¹*Department of Physics and Astronomy, University of Tennessee - Knoxville, Knoxville, TN*

²*Oak Ridge National Laboratory, Oak Ridge, TN*

³*Department of Materials Science and Engineering,
University of Tennessee - Knoxville, Knoxville, TN*

⁴*Advanced Photon Source, Argonne National Laboratory, Darien, IL*

(Dated: November 8, 2018)

In this work we present the results of an inelastic x-ray scattering experiment detailing the behavior of the transverse acoustic [110] phonon in BaFe_2As_2 as a function of temperature. When cooling through the structural transition temperature, the transverse acoustic phonon energy is reduced from the value at room temperature, reaching a maximum shift near inelastic momentum transfer $\vec{q} = 0.1$. This softening of the lattice results in a change of the symmetry from tetragonal to orthorhombic at the same temperature as the transition to long-range antiferromagnetic order. While the lattice distortion is minor, the anisotropy in the magnetic exchange constants in pnictide parent compounds is large. We suggest mechanisms of electron-phonon coupling to describe the interaction between the lattice softening and onset of magnetic ordering.

PACS numbers: 63.20.-e, 74.25.kc, 63.20.kd

I. INTRODUCTION

Discovery of superconductivity in iron pnictide materials¹ spurred intense experimental and theoretical effort to unravel the underlying physics of these compounds. The presence of FePn_4 tetrahedra is universal in pnictide compounds, where iron atoms are arranged in a square planar lattice and tetrahedrally coordinated by pnictogen atoms. A common dynamic feature in pnictide families is a structural phase transition concomitant or in close vicinity with a transition to long range antiferromagnetic (AFM) order upon cooling^{2,3}. This transition is suppressed with hole⁴⁻⁶, electron^{7,8}, or isoelectronic doping^{9,10}, eventually giving way to superconductivity.

At room temperature, the pnictide parent compound BaFe_2As_2 is a tetragonal ($I4/mmm$) paramagnet. At $T \approx 140 \text{ K}$, BaFe_2As_2 undergoes a structural transition to orthorhombic ($Fmmm$) symmetry, and magnetically orders with spins AFM along the a -axis in the iron plane, ferromagnetic along the b -axis, and AFM between the iron layers with an ordered moment of $0.87(3) \mu_B$ per Fe site¹¹. The measured moment is lower than that predicted by DFT calculations¹². While the structural distortion in the pnictides is small, the magnetic exchange anisotropy is very large when the exchange constants are calculated from an anisotropic Heisenberg model calculation which includes damping with very small interlayer magnetic coupling^{13,14}.

For AFM ordering to occur, the high temperature tetragonal symmetry of BaFe_2As_2 must be broken to allow for the spin anisotropy, making the lattice distortion from tetragonal to orthorhombic symmetry a requirement for AFM ordering. The precise mechanism of the lattice distortion is a matter of considerable debate¹⁵⁻²².

Early theoretical work shows that the lattice

distortion² in the oxyarsenide LaFeAsO is the manifestation of relieved magnetic frustrations as the AFM ordering results in different occupancy for the d_{xz} , d_{yz} orbitals which breaks the tetragonal symmetry²⁰. However, the exchange constants determined from the spin wave dispersion are not consistent with this idea¹³. Another explanation for the coupling of the transitional behaviors is that of ferro-orbital ordering. A minimal approach applying the Hartree-Fock approximation to a two orbital model shows that AFM ordering arises as a consequence of ferro-orbital ordering, which then results in a lattice distortion²³. Three- and five-orbital models suggest that orbital degrees of freedom are strongly coupled to magnetic ordering, with d_{xz} and d_{yz} susceptible to orbital ordering, but that the orbital magnetization is much greater for the d_{yz} orbital, resulting in a reduction of the orbital hybridization between the d_{xz} and d_{yz} orbitals²⁴. Other reports suggest that orbital ordering is able to spontaneously break the C_4 symmetry locally without Fermi surface nesting or magnetic frustrations²¹.

Softening of the shear elastic constant in $\text{Ba}(\text{Fe}_x\text{Co}_{1-x})_2\text{As}_2$ has been noted in several works including resonant ultrasound spectroscopy on BaFe_2As_2 and $\text{Ba}(\text{Fe}_{0.92}\text{Co}_{0.08})_2\text{As}_2$,²⁵ and ultrasonic pulse echo measurements on undoped, underdoped²⁶, and optimally doped $\text{Ba}(\text{Fe}_x\text{Co}_{1-x})_2\text{As}_2$ ¹⁶. The measurements showed a softening of the C_{66} mode near the structural or superconducting transition in all compounds where measurement wasn't precluded by sample instability against the mounting apparatus. The C_{66} mode is responsible for structural phase transitions of type which serve to lower crystalline symmetry from tetragonal to orthorhombic^{27,28}, so this observation is expected, although in the presented works several additional mechanisms for the phase transition are proffered.

Resonant ultrasound spectroscopy measurements per-

formed on BaFe_2As_2 show a strong softening of the shear elastic constant, which is used to conclude that there is general lattice softening through the structural transition driven by renormalization of the shear elastic constant by nematic fluctuations²⁵. In this context, the softening of the lattice is a secondary effect, with electronic degrees of freedom taking precedence over elastic, and the structural transition then a mere consequence of the magnetic ordering. In the work conducted in ultrasonic pulse echo spectroscopy, the softening minima tracks with the superconducting temperature under application of a magnetic field^{16,26}, and other elastic constants show almost imperceptible deviations from monotonic behavior in close proximity to the superconducting transition temperature¹⁶. One hypothesis derived from these experiments is the phase transition is driven by ferro-orbital ordering, suggestive of strong lattice coupling and orbital fluctuations²⁶, while another concludes that the softening is induced by the coupling of the degenerate electronic orbitals to the elastic strain¹⁶.

There is some disagreement between the reports on the elastic constant behavior at low temperature. Upon cooling below the structural or superconducting temperature, some reports show the value of C_{66} recovering some 10% of the room temperature value at low temperature for the undoped and superconducting samples²⁵, while other reports on the underdoped show no further observed softening below the structural transition temperature¹⁶.

Experimental studies on the transverse acoustic (TA) modes of the related compound CaFe_2As_2 shows a softening of the transverse acoustic mode at the zone boundary for a TA [110] mode, and a mid-zone point at TA [100] at the magneto-structural transition when measuring accompanied by phonon broadening²⁹. Further, calculation shows that phonons are very sensitive to the structural details of the FePn_4 layers, with phonon modes that distort the tetrahedra having substantial impact on the electronic density of states close to E_F ³⁰. Anomalous phonon behavior is observed in Raman spectroscopy, with the E_g in-plane phonon mode split in BaFe_2As_2 ³¹⁻³³, which is linked to strong spin-phonon coupling. This E_g mode is a doubly-degenerate mode impacting Fe and As, and the contention is that the split is too large to be accounted for by the orthorhombic distortion and instead is indicative of spin-phonon coupling. Measurements of phonon behavior conducted with inelastic x-ray spectroscopy are replicated well by theory when magnetism is explicitly taken into account³⁴, indicating the presence of spin-phonon coupling.

The degree of hybridization between the As-4*p* and Fe-3*d* states is shown to have strong impacts on the Fe^{2+} spin state³⁵, and to influence the Fe-As phonon modes²¹. Further, the dependence of the superconducting critical temperature^{36,37} and magnetic moment^{38,39} of pnictide materials as a function of Fe-As layer separation is well established.

The preceding discussion sets forth a clear need to understand the specifics of the structural transition as they

relate to the elastic degrees, magnetic, and orbital degrees of freedom. Here we report the results of inelastic x-ray spectroscopy (IXS) measurements on single crystals of BaFe_2As_2 as a function of temperature. Since the acoustic phonon frequency goes as the square root of the elastic constant, we expect a softening of the low-energy acoustic phonon modes of BaFe_2As_2 when passing through the structural transition temperature. Phonon calculations predict a linear dispersion in the low-energy, long wavelength regime^{30,34}. The acoustic phonon modes in BaFe_2As_2 can be characterized with energy transfers of less than 10 meV, and the small and constant momentum resolution offered by IXS allows precise measurements of the phonon dispersion as a function of temperature. The previous measurements on the shear elastic constant²⁵ provide information only at the zone center (Γ point, $\vec{q} = 0$), so the IXS measurements described in this work provide additional information on the low-energy lattice dynamics in the BaFe_2As_2 system.

II. EXPERIMENT

We investigated the behavior of the transverse acoustic phonon mode in BaFe_2As_2 near the $(2,2,0)_O$ position, which is the [110] mode in the reduced scheme. The orthorhombic notation and the $Fmmm$ symmetry are used throughout this report. The measurements were made using the HERIX instrument on beamline 3-ID of the Advanced Photon Source at Argonne National Laboratory^{40,41}. The HERIX instrument is an insertion device beamline with a six-bounce monochromator setup providing an incident energy of 21.657 keV, and a resolution of 2.3 meV at the elastic line.

Our sample was a single crystal of BaFe_2As_2 measuring 1mm x 2mm x 60 μm , grown using a self-flux method⁷. Calculated optimal thickness for a transmission mode geometry for an incident energy of 21.657 keV was 55 μm . The crystal was oriented in transmission mode with $(2, 2, 0)$ and $(1, 1, 3)$ in the scattering plane. This alignment allows measurement of the phonons in the basal plane of the form $\vec{Q} = \vec{G} + \vec{q} = (\vec{H} - \vec{q}, \vec{K} + \vec{q})$, where $\vec{G} = (\vec{H}, \vec{K})$ is the reciprocal lattice vector of the Bragg peak in the $a - b$ plane, and \vec{q} the inelastic momentum transfer. For temperature dependent studies, the crystal samples were mounted on copper holders with a small amount of varnish, and the copper holders were attached to the cold finger of a closed cycle cryostat sealed by a beryllium dome.

The beam size on sample was 50 μm by 350 μm . Only one analyzer-detector pair was used for these measurements, and an analyzer mask was used to limit Bragg contamination for low \vec{q} measurements. The mask size was 4 cm by 4 cm at $\vec{q} \geq 0.07$, and 1 cm by 1 cm for all $\vec{q} < 0.07$. The Stokes and anti-Stokes profiles were measured in most cases, but at points where an anti-Stokes contribution to the phonon spectra was dynamically limited, a contribution from elastic scattering was ensured

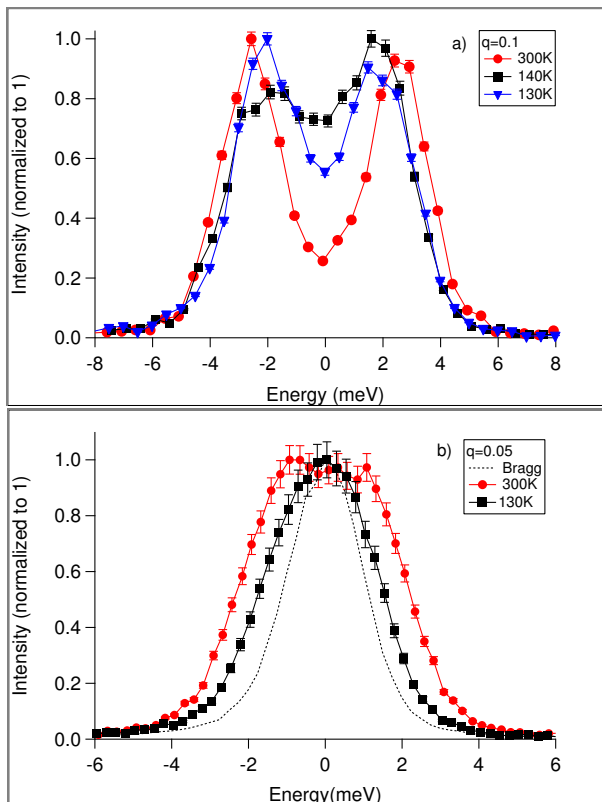


FIG. 1. (Color online) a) Comparison of 300 K, 140 K, and 130 K phonon spectra at $\vec{q} = 0.1$. b) Comparison of 300 K and 130 K phonon spectra at $\vec{q} = 0.05$. The dotted line shows the Bragg peak measurement at $T=130$ K, $\vec{Q}=(2,2,0)_O$. All spectra are Bose factor corrected and normalized to one. Errors are statistical errors propagated through Bose correction.

by transversely scanning the crystal space at zero energy transfer. All data were normalized to the incident monitor count, a low efficiency ion chamber.

For all temperatures, the phonon spectra were fit with Voigt profiles, employing the Whiting approximation to determine the width^{42,43}. Phonon spectra were corrected for the Bose thermal population factors.

Fitted phonon peak widths are constrained to that of a phonon measured at $\vec{q} = 0.2$ at $T = 130$ K. Data for values of $\vec{q} > 0.07$ were fit with two phonon peaks and an elastic contribution. The phonon energy for $\vec{q} > 0.07$ is determined by the average of the fitted peak positions of the Stokes and anti-Stokes contributions.

Data for $\vec{q} \leq 0.07$ at temperatures below 300 K can not be resolved as distinct peaks, so the width of the observed peak is used as a proxy for the degree of softening (Fig. 1). The peak width is determined using a single Voigt profile.

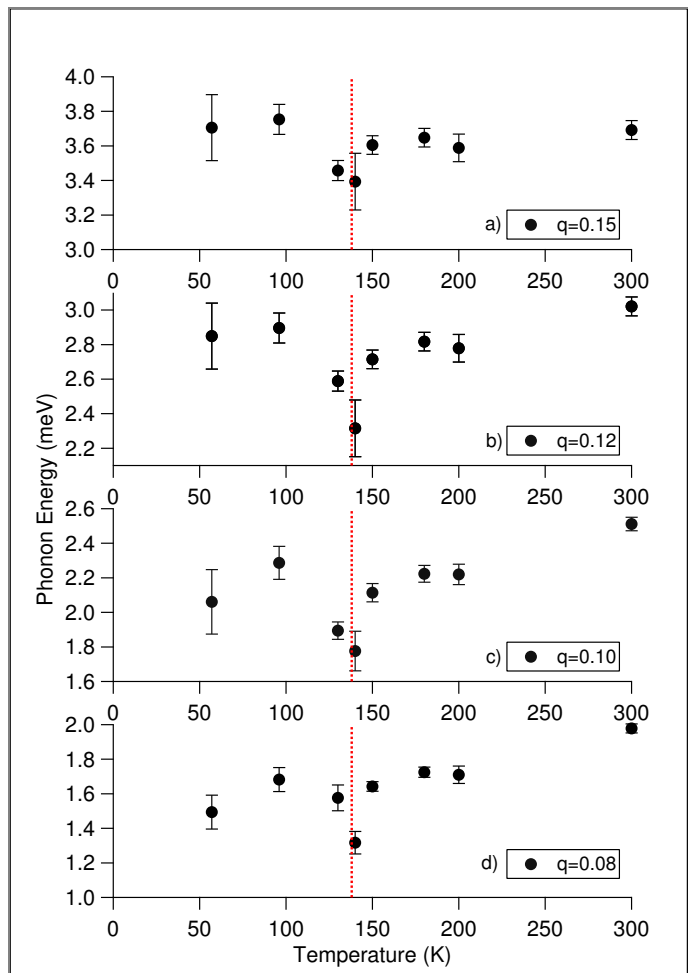


FIG. 2. (Color online) Energy of transverse acoustic phonon as a function of temperature for $\vec{Q} = (\vec{H} - \vec{q}, \vec{K} + \vec{q})$ for $H = K = 2$ and $\vec{q} =$ (a) 0.15, (b) 0.12, (c) 0.10, (d) 0.08 in orthorhombic reciprocal lattice units. Dotted line indicates T_S . Error bars are statistical errors propagated through Bose correction and peak averaging. Two softenings are observed, one at T_S and additional softening at low \vec{q} at low temperature.

III. DISCUSSION

The primary result of our investigation is the observation of a reduction in energy of the $[110]_O$ transverse acoustic phonon in the low \vec{q} region, evident from the measured phonon spectra (Fig. 1). The data show this reduction is most pronounced at $\vec{q} = 0.1$, reaching a maximal amount near $T = 140$ K (Fig. 2). As the temperature is decreased, the phonon energy decreases, and then recovers, but not to the full energy observed at room temperature (Fig. 2) before decreasing again at low temperatures and low \vec{q} .

For data with $\vec{q} \leq 0.07$ the fitted width of the peak centered around zero energy transfer exhibits a linear behavior for 300 K (Fig. 3a), with the width of the spectra collapsing into the Bragg peak width for lower tempera-

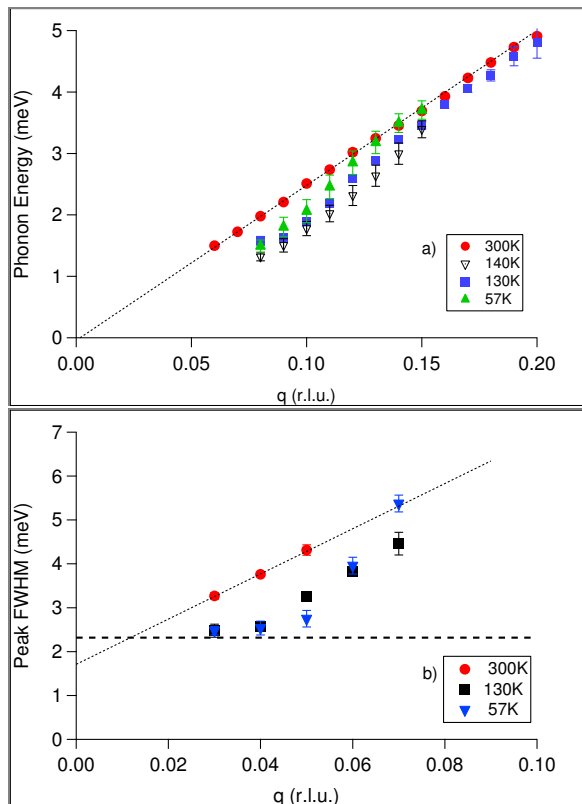


FIG. 3. (Color online) a) Dispersion of TA phonon at 300 K, 140 K, 130 K, and 57 K. Dotted line indicates a linear fit to the 300K data. b) Central peak width as a function of \vec{q} for $T=300$ K, 130 K, and 57 K. Heavy dashed line at $E = 2.3$ meV indicates the width of the Bragg peak measured at $\vec{Q} = (2, 2, 0)$ $T=130$ K. Dotted line on 300 K data represents the fitted peak width. Error bars are statistical errors propagated through Bose correction and the curve fitting procedure.

tures (Fig. 3b).

The lattice softening observed in the shear elastic measurements show a drop in the shear mode to a minimal values at T_S , and then a slight recovery to low temperatures^{16,25}, or no recovery at all²⁶. This is in contrast to our observations here, as the phonon energy recovers most of the energy after softening, and the slope of the dispersion changes at low temperature.

The only mode investigated in this work was the low energy transverse acoustic mode, and there was only a local softening of the mode - the traditional linear dispersion is recovered by $\vec{q} = 0.20$ in all temperature cases (four temperature cases shown in Fig. 3). This result is not captured in published DFT-GGA calculations reviewed in preparation of this manuscript.

The softening of the low energy transverse acoustic mode observed by IXS is expected in the context of soft mode transitions, as the decrease in energy of the long wavelength phonons is always seen in structural phase transitions of the type observed here²⁷. But it has a few possible interpretations for microscopic mechanism.

The first interpretation invokes Fermi surface nesting,

which results in a regime of enhanced electron-phonon coupling. The Fermi surface structure of pnictides is well established to consist of hole pockets centered at the zone center, and electron pockets at the zone boundary^{44,45}, with electron or hole doping serving to change the levels of the two pockets relative to one another⁴⁶. The softening of the TA phonon has a natural explanation in two-dimensional Fermi surface nesting giving rise to a Kohn anomaly, where strong quasiparticle excitations below $\vec{q} = 2k_F$ result in enhanced electron-phonon coupling⁴⁷. Indeed we observe softening from the zone center to a maximal phonon softening below $\vec{q} = 0.1$, which is consistent with the value of $2k_F = 0.1$ for the inner hole pocket in BaFe_2As_2 ⁴⁸.

In a work on CaFe_2As_2 , a series of line broadenings is observed²⁹, though this is not used to draw the conclusion of Kohn anomalies, but may be related to the work here. However, possible broadening of the phonons for the BaFe_2As_2 compound studied here is too small to be fully resolved by the current technique. Line broadenings of this type have been observed in studies of elemental superconductors, where the phonon anomalies were fully resolved only when using high resolution spin-echo neutron spectroscopy⁴⁹. In order to confirm the presence of phonon broadening and/or a Kohn anomaly in BaFe_2As_2 , a careful analysis of the phonon lineshape using a higher energy resolution is required. Note also that there is some softening tendency at temperatures much below T_S . The \vec{q} range of this low temperature softening is distinct from the softening at T_S ; below $\vec{q} = 0.12$ at low temperatures, whereas softening is observed below $\vec{q} = 0.16$ near T_S . It appears that this softening has a different origin, and either one could be related to a Kohn anomaly.

A second interpretation is to consider the phonon softening in the context of coupling between the low energy acoustic mode and the orbital fluctuations. In this scenario, softening of the shear mode causes in-plane shifting of the iron atoms, impacting the interatomic distances along the FePn_4 layer. As these atoms shift their positions, the tetragonal orbital degeneracy between the d_{xz} and d_{yz} orbitals is broken, allowing the manifestation of magnetic order. While the orthorhombic structural distortion is small (of order 0.3%, with the change in the iron square lattice 2.8 \AA on a side to a rectangle $2.79/2.81 \text{ \AA}$), and several works show that there is a strong dependence of the electronic structure on small details of the lattice, in particular the height of the pnictogen atom above the iron plane^{44,52}. Additionally, it has been shown that there is an enhancement of electron-boson coupling arising from orbital anisotropy²¹, behavior which is in contrast to lower mean field values for the estimate of such couplings^{50,51}. Further, the pnictide systems are very close to the Stoner criticality, where even a small lattice distortion can have a large consequence to the magnetism in the system³⁹.

The proposed mechanism indicates that other phonon modes may be involved in the structural transition via a similar softening behavior³⁹. Modes that directly in-

fluence the dynamics of the FeAs_4 tetrahedra are being examined. Further, a coupling of acoustic and optical modes as is seen in other structural phase transitions⁵³ is not ruled out, and requires further examination.

IV. CONCLUSIONS

We have investigated the behavior of the transverse acoustic phonon in BaFe_2As_2 using IXS, and found that this phonon mode softens as a function of temperature, with a maximal softening near $\bar{q} = 0.1$. The energy of the phonon mode drops well below that observed at room temperature, reaching a minimum near the structural phase transition temperature before recovering almost

fully. This observation is explained in terms of electron-phonon coupling resulting in a lifting of the orbital degeneracy in the paramagnetic tetragonal state, allowing full manifestation of the AFM order.

ACKNOWLEDGMENTS

This work was supported by the Office of Basic Sciences, US Department of Energy through the EPSCoR grant, DE-FG02-08ER46528 (JN, DP, KL and TE), and the Basic Energy Sciences, Materials Sciences and Engineering (AS). This work at the Advanced Photon source was supported by the U.S. Department of Energy, Office of Science, Office of Basic Energy Sciences, under Contract no DE-AC02-06CH11357.

-
- * jniedzie@utk.edu
 † Present Address Department of Physics, University of Colorado, Boulder, CO, 80302.
- ¹ Y. Kamihara, T. Watanabe, M. Hirano, and H. Hosono, *J. Am. Chem. Soc.* **130**, 3296 (2008).
 - ² C. de la Cruz, Q. Huang, J. W. Lynn, J. Li, W. R. Li, J. L. Zarestky, H. A. Mook, G. F. Chen, J. L. Luo, N. L. Wang, et al., *Nature* **453**, 899 (2008).
 - ³ M. Rotter, M. Tegel, D. Johrendt, I. Schellenberg, W. Hermes, and R. Pottgen, *Phys. Rev. B* **78**, 020503(R) (2008).
 - ⁴ H. Takahashi, K. Igawa, K. Arii, Y. Kamihara, M. Hirano, and H. Hosono, *Nature* **453**, 376 (2008).
 - ⁵ X. H. Chen, T. Wu, G. Wu, R. H. Liu, H. Chen, and D. F. Fang, *Nature* **453**, 761 (2008).
 - ⁶ M. Rotter, M. Tegel, and D. Johrendt, *Phys. Rev. Lett.* **101**, 107006 (2008).
 - ⁷ A. S. Sefat, R. Jin, M. A. McGuire, B. C. Sales, D. J. Singh, and D. Mandrus, *Phys. Rev. Lett.* **101**, 117004 (2008).
 - ⁸ A. S. Sefat, A. Huq, M. A. McGuire, R. Jin, B. C. Sales, D. Mandrus, L. M. D. Cranswick, P. W. Stephens, and K. H. Stone, *Phys. Rev. B* **78**, 104505 (2008).
 - ⁹ Z. Ren, Q. Tao, S. Jiang, C. Feng, C. Wang, J. Dai, G. Cao, and Z. Xu, *Phys. Rev. Lett.* **102**, 137002 (2009).
 - ¹⁰ S. Jiang, H. Xing, G. Xuan, C. Wang, Z. Ren, C. Feng, J. Dai, Z. Xu, and G. Gao, *J. Phys.: Condens. Matter* **21**, 382203 (2009).
 - ¹¹ Q. Huang, Y. Qiu, W. Bao, M. A. Green, J. W. Lynn, Y. C. Gasparovic, T. Wu, G. Wu, and X. H. Chen, *Phys. Rev. Lett.* **101**, 257003 (2008).
 - ¹² M. Lumsden and A. Christianson, *J. Phys.: Condens. Matter* **22**, 23203 (2010).
 - ¹³ J. Zhao, D. T. Adroja, D.-X. Yao, R. Bewley, S. Li, X. F. Wang, G. Wu, X. H. Chen, J. Hu, and P. Dai, *Nature Physics* **5**, 555 (2009).
 - ¹⁴ L. W. Harriger, H. Q. Luo, M. S. Liu, C. Frost, J. P. Hu, M. R. Norman, and P. Dai, *Phys. Rev. B* **84**, 054544 (2011).
 - ¹⁵ H. Kontani, T. Saito, and S. Onari, *Phys. Rev. B* **84**, 024528 (2011).
 - ¹⁶ T. Goto, R. Kurihara, K. Araki, K. Mitsumoto, M. Akatsu, Y. Nemoto, S. Tatematsu, and M. Sato, *J. Phys. Soc. Japan* **80**, 073702 (2011).
 - ¹⁷ I. Paul, *Phys. Rev. Lett.* **107**, 047004 (2011).
 - ¹⁸ M. D. Johannes, I. I. Mazin, and D. S. Parker, *Phys. Rev. B* **82**, 024527 (2010).
 - ¹⁹ M. D. Johannes and I. I. Mazin, *Phys. Rev. B* **79**, 220510 (2009).
 - ²⁰ T. Yildirim, *Physica C* **469**, 425 (2009).
 - ²¹ C.-C. Lee, W.-G. Yin, and W. Ku, *Phys. Rev. Lett.* **103**, 267001 (2009).
 - ²² H. Kontani and S. Onari, *Phys. Rev. Lett.* **104**, 157001 (2010).
 - ²³ K. Kubo and P. Thalmeier, *J. Phys. Soc. Japan* **78**, 3704 (2009).
 - ²⁴ M. Daghofer, Q. L. Luo, R. Yu, D. X. Yao, A. Moreo, and E. Dagotto, *Phys. Rev. B* **81**, 180514 (2010).
 - ²⁵ R. M. Fernandes, L. H. VanBebber, S. Bhattacharya, P. Chandra, V. Keppens, D. Mandrus, M. A. McGuire, B. C. Sales, A. S. Sefat, and J. Schmalian, *Phys. Rev. Lett.* **105**, 157003 (2010).
 - ²⁶ M. Yoshizawa, R. Kamiya, R. Onodera, Y. Nakanishi, K. Kihou, H. Eisaki, and C. H. Lee, *arXiv cond-mat.supr-con* (2010), 1008.1479v3.
 - ²⁷ R. A. Cowley, *Structural Phase Transitions* (1976).
 - ²⁸ R. Folk, H. Iro, and F. Schwabl, *Z. Phys. B* **25**, 69 (1976).
 - ²⁹ R. Mittal, L. Pintschovius, D. Lamago, R. Heid, K. P. Bohnen, D. Reznik, S. Chaplot, Y. Su, N. Kumar, S. Dhar, et al., *Phys. Rev. Lett.* **102**, 217001 (2009).
 - ³⁰ M. Zbiri, H. Schober, M. R. Johnson, S. Rols, R. Mittal, Y. Su, M. Rotter, and D. Johrendt, *Phys. Rev. B* **79**, 064511 (2009).
 - ³¹ L. Chauviere, Y. Gallais, M. Cazayous, A. Sacuto, M. A. Méasson, D. Colson, and A. Forget, *Phys. Rev. B* **80**, 94504 (2009).
 - ³² A. A. Schafgans, B. C. Pursley, A. D. LaForge, A. S. Sefat, D. Mandrus, and D. N. Basov, *Phys. Rev. B* **84**, 052501 (2011).
 - ³³ M. Rahlenbeck, G. L. Sun, D. L. Sun, C. T. Lin, B. Keimer, and C. Ulrich, *Phys. Rev. B* **80**, 064509 (2009).
 - ³⁴ D. Reznik, K. Lokshin, D. C. Mitchell, D. Parshall, W. Dmowski, D. Lamago, R. Heid, K.-P. Bohnen, A. S. Sefat, M. A. McGuire, et al., *Phys. Rev. B* **80**, 214534 (2009).
 - ³⁵ T. Yildirim, *Phys. Rev. Lett.* **102**, 037003 (2009).

- ³⁶ C.-H. Lee, A. Iyo, H. Eisaki, H. Kito, M. T. Fernandez-Diaz, T. Ito, K. Kihou, H. Matsuhata, M. Braden, and K. Yamada, *J. Phys. Soc. Jpn.* **77**, 083704 (2008).
- ³⁷ Y. Mizuguchi, Y. Hara, K. Deguchi, S. Tsuda, T. Yamaguchi, K. Takeda, H. Kotegawa, H. Tou, and Y. Takano, *Supercond Sci Tech* **23**, 054013 (2010).
- ³⁸ C. de la Cruz, W. Z. Hu, S. Li, Q. Huang, J. W. Lynn, M. A. Green, G. F. Chen, N. L. Wang, H. A. Mook, Q. Si, et al., *Phys. Rev. Lett.* **104**, 017204 (2010).
- ³⁹ T. Egami, B. V. Fine, D. Parshall, A. Subedi, and D. J. Singh, *Adv. Cond. Mat. Physics* **2010**, 164916 (2010).
- ⁴⁰ T. S. Toellner, A. Alatas, A. Said, D. Shu, W. Sturhahn, and J. Zhao, *J. Synchrotron Radiat.* **13**, 211 (2006).
- ⁴¹ H. Sinn, E. E. Alp, A. Alatas, J. Barraza, G. Bortel, E. Burkel, D. Shu, W. Sturhahn, J. P. Sutter, T. S. Toellner, et al., *Nucl. Instrum. and Meth.* **467-468**, 1545 (2001).
- ⁴² E. Whiting, *Journal of Quantitative Spectroscopy and Radiative Transfer* **8**, 1379 (1968).
- ⁴³ J. Olivero and R. Longbothum, *Journal of Quantitative Spectroscopy and Radiative Transfer* **17**, 233 (1977).
- ⁴⁴ D. J. Singh, *Phys. Rev. B* **78**, 094511 (2008).
- ⁴⁵ C. Liu, T. Kondo, R. M. Fernandes, A. D. Palczewski, E. D. Mun, N. Ni, A. N. Thaler, A. Bostwick, E. Rotenberg, J. Schmalian, et al., *Nature Physics* **6**, 419 (2010).
- ⁴⁶ B. C. Sales, M. A. McGuire, A. S. Sefat, and D. Mandrus, *Physica C* **470**, 304 (2010).
- ⁴⁷ W. Kohn, *Phys. Rev. Lett.* **2**, 393 (1959).
- ⁴⁸ V. Brouet, M. Marsi, B. Mansart, A. Nicolaou, A. Taleb-Ibrahimi, P. L. LeFèvre, F. Bertran, F. Rullier-Albenque, A. Forget, and D. Colson, *Phys. Rev. B* **80**, 165115 (2009).
- ⁴⁹ P. Aynajian, T. Keller, L. Boeri, S. M. Shapiro, K. Habicht, and B. Keimer, *Science* **319**, 1509 (2008).
- ⁵⁰ L. Boeri, O. V. Dolgov, and A. A. Golubov, *Phys. Rev. Lett.* **101**, 026403 (2008).
- ⁵¹ L. Boeri, M. Calandra, I. I. Mazin, O. V. Dolgov, and F. Mauri, *Phys. Rev. B* **82**, 020506(R) (2010).
- ⁵² D. J. Singh and M. H. Du, *Phys. Rev. Lett.* **100**, 237003 (2008).
- ⁵³ S. M. Shapiro, *Appl. Phys. A*, **99**, 543 (2010).